Defence Research and Development Canada	Recherche et développement pour la défense Canada

DEFENCE R&D DÉFENSE

Focusing ISAR Images using Adaptive Joint Time-Frequency Algorithm on Simulated and Experimental Radar Data

T. Thayaparan, S.K. Wong, E. Riseborough
and G. Lampropoulos

Defence R&D Canada – Ottawa
TECHNICAL MEMORANDUM
DRDC Ottawa TM 2003-089
March 2003

Canada

Focusing ISAR images using adaptive joint time-frequency algorithm on simulated and experimental radar data

T. Thayaparan, S. K. Wong, E. Riseborough
Defence R&D Canada - Ottawa

G. Lampropoulos
A.U.G. Signals Ltd

Defence R&D Canada - Ottawa

Technical Memorandom

DRDC Ottawa TM 2003-089

March 2003

Abstract

When target motion is confined to a two-dimensional plane during coherent processing intervals, the adaptive joint time-frequency algorithm is shown to be an effective method for achieving rotational motion compensation in ISAR imaging. We illustrate the algorithm using both simulated and measured experimental radar data sets. The results show that the adaptive joint time-frequency algorithm performed very well in achieving a focused image of the target. Results also demonstrate that adaptive joint time-frequency techniques can significantly improve the distorted ISAR image over what can be achieved by conventional Fourier transform methods when the rotational motion of the target is confined to a two-dimensional plane. This study also adds insight into the distortion mechanisms that affect the ISAR images of a target in motion.

Résumé

On a constaté, lorsque le mouvement d'un objectif est confiné à un espace bidimensionnel (plan) dans des intervalles de traitement cohérent, que l'algorithme temps-fréquence mixte adaptatif constitue un outil efficace pour réaliser la compensation de mouvement de rotation en imagerie ISAR. Nous illustrons le fonctionnement de l'algorithme à l'aide d'ensembles de données radar obtenus tant par simulation que par des mesures expérimentales. Les résultats montrent que l'algorithme temps-fréquence mixte adaptatif a été très efficace pour la production d'une image mise au point de l'objectif. Ils montrent également que les techniques temps-fréquence mixtes adaptatives permettent d'améliorer l'image ISAR déformée beaucoup mieux que les méthodes à transformation de Fourier classiques lorsque le mouvement de rotation de l'objectif est confiné à un espace bidimensionnel. La présente étude permet en outre de mieux comprendre les mécanismes de déformation qui influent sur les images ISAR d'un objectif en mouvement.

This page intentionally left blank.

Executive summary

Inverse Synthetic Aperture Radar (ISAR) imaging has been around for many years and is used in microwave radar applications such as signature diagnostic and target identification applications. ISAR images of aircraft can provide functional target signatures for Non-Cooperative Target Recognition (NCTR). The problem of NCTR has always been a topic of interest in military operations, that is, to improve situational awareness. Therefore the ability to generate focused images from ISAR systems is of paramount importance to military and intelligence operations. Since the image is a two-dimensional projection of the target, spatial features present in the ISAR images have the potential of offering sufficient information about the targets for identification purposes.

When an aircraft is in motion, small random perturbing rotational motions in pitch, roll and yaw are often produced. Unfortunately, these perturbed motions introduce distortion (e.g., blurring) in the ISAR images. The observation of very large distortions from experimental ISAR data has been reported. These observations clearly show that whenever an aircraft has a complex motion, such as pitching, yawing, rolling, the resulting ISAR image becomes severely distorted. It is very difficult to conduct a definitive study on the distortion phenomenon using in-flight aircraft. For example, there is no information on the location of the target rotational axis and no prior knowledge of the true (static) image of the target for comparison with the analysis. Therefore, we conducted a set of controlled experiments on the distortion of ISAR images in order to perform a systematic analysis of ISAR images. A numerical model was developed to simulate the distorted ISAR images due to various time-dependent rotational motions that can occur in real in-flight targets. This will allow us to gain new insights and a better understanding of the distortion phenomenon.

In this paper, an adaptive joint time-frequency algorithm has been applied and evaluated for focusing distorted ISAR (inverse synthetic aperture radar) images when the target motion is confined to a two-dimensional plane. It is shown that the adaptive joint time-frequency algorithm provides an effective method of achieving rotational motion compensation for ISAR imaging. Examples provided demonstrate the effectiveness of the adaptive joint time-frequency algorithm with both simulated and experimental ISAR data. Results show that if a target is moving smoothly, standard motion compensation generates a clear image of the target by using the conventional Fourier transform methods. However, when a target performs complex motion such as perturbed random motions, standard motion compensation is not sufficient to generate an acceptable image. In this case, the adaptive joint time-frequency algorithm provides an efficient candidate to resolve the image smearing caused by the time-varying behavior and leads to a well-focused ISAR image when the target motion is confined to a two-dimensional plane. This study also adds insight into the distortion mechanisms that affect the ISAR images of a target in motion.

T. Thayaparan, S. K. Wong, E. Riseborough, G. Lampropoulos. 2003. Focusing ISAR images

using adaptive joint time-frequency algorithm on simulated and experimental radar data. DRDC Ottawa TM 2003-089. Defence R&D Canada - Ottawa.

Sommaire

L’imagerie par radar à synthèse d’ouverture inverse (ISAR) existe depuis un bon nombre d’années et elle est utilisée dans les applications du radar hyperfréquence, par exemple pour la reconnaissance de signature et l’identification des objectifs. Les images ISAR d’un aéronef peuvent fournir des signatures fonctionnelles d’objectif pour la reconnaissance des objectifs non coopératifs (NCTR). Le problème de la NCTR a toujours suscité l’intérêt dans les opérations militaires, par exemple pour améliorer la connaissance de la situation. Par conséquent, la capacité de générer des images mises au point à l’aide des systèmes ISAR est d’une importance primordiale pour les opérations militaires et les opérations de renseignement. Comme l’image est une projection bidimensionnelle de l’objectif, les caractéristiques spatiales présentes dans les images ISAR peuvent fournir suffisamment d’information sur les objectifs pour permettre l’identification.

Lorsqu’un aéronef est en déplacement, de petits mouvements de rotation perturbateurs en tangage, en roulis et en lacet sont souvent produits. Malheureusement, ces mouvements perturbateurs créent une distorsion (p. ex. flou) des images ISAR. On a signalé que des distorsions très importantes avaient été observées à partir de données ISAR expérimentales. Les observations faites montrent clairement que dans le cas d’un aéronef effectuant un mouvement complexe, par exemple avec tangage, lacet et roulis, l’image ISAR résultante est grandement déformée. Il est très difficile de mener une étude définitive du phénomène de distorsion à l’aide d’un aéronef en vol. Par exemple, on ne dispose pas de données sur la position de l’axe de rotation de l’objectif ni de connaissance préalable de l’image (statique) vraie de l’objectif pour fins de comparaison avec l’analyse. Nous avons donc réalisé un ensemble d’expériences contrôlées sur la distorsion des images ISAR dans le but d’effectuer une analyse systématique des images ISAR. Nous avons élaboré un modèle numérique pour simuler les images ISAR déformées en raison des divers mouvements de rotation dépendants du temps qui peuvent se produire dans le cas d’objectifs réels en vol. Nous pourrons ainsi acquérir de nouvelles connaissances et mieux comprendre le phénomène de distorsion.

Le présent document traite de l’application et de l’évaluation d’un algorithme temps-fréquence mixte adaptatif pour la mise au point d’images ISAR (radar à synthèse d’ouverture inverse) déformées lorsque le mouvement de l’objectif est limité à un espace bidimensionnel (plan). On montre que l’algorithme temps-fréquence mixte adaptatif constitue un outil efficace pour réaliser la compensation de mouvement de rotation en imagerie ISAR. Les exemples fournis montrent l’efficacité de l’algorithme temps-fréquence mixte adaptatif tant avec des données ISAR simulées qu’avec des données ISAR expérimentales. Les résultats obtenus montrent, dans le cas d’un objectif se déplaçant de façon régulière, que la compensation de mouvement normale donne une image claire de l’objectif à l’aide des méthodes à transformation de Fourier classiques. Cependant, lorsqu’un objectif effectue un mouvement complexe, par exemple un mouvement aléatoire perturbé, la compensation de mouvement normale n’est pas suffisante pour produire une image acceptable. Dans ce cas, l’algorithme temps-fréquence mixte adaptatif constitue un candidat efficace pour corriger les défauts de l'image attribuables au comportement dépendant du temps et permet d'obtenir une image ISAR bien mise au point lorsque le mouvement de l'objectif est confiné dans un espace bidimensionnel. Cette étude permet aussi de mieux comprendre les mécanismes de distorsion qui influent sur les images ISAR d'un objectif en mouvement.

T. Thayaparan, S. K. Wong, E. Riseborough, G. Lampropoulos. 2003. Focusing ISAR images using adaptive joint time-frequency algorithm on simulated and experimental radar data. DRDC Ottawa TM 2003-089. R & D pour la defénse Canada - Ottawa.

Table of contents

List of figures

1. Introduction

Inverse Synthetic Aperture Radar (ISAR) imaging has been around for many years and is used in microwave radar applications such as signature diagnostic and target identification applications. ISAR images of aircraft can provide functional target signatures for Non-Cooperative Target Recognition (NCTR) [1-2]. The problem of NCTR has always been a topic of interest in military operations, that is, to improve situational awareness. Therefore the ability to generate focused images from ISAR systems is of paramount importance to military and intelligence operations. Since the image is a two-dimensional projection of the target, spatial features present in the ISAR images have the potential of offering sufficient information about the targets for identification purposes [1-2].

One of the main challenges in ISAR image formation is the unknown nature of the target motion. The essential requirement for ISAR imaging is target rotation. This type of motion produces the Doppler shift required to map the target's reflectivity in the cross-range direction. However, to form an image using the conventional two-dimensional discrete Fourier transform approach, target rotation must be small to avoid blurring of image features. Blurring or image defocusing is caused by a combination of a varying cross-range and range walk. Time-varying Doppler shifts associated with the individual target scattering points must be smaller than the Doppler resolution to prevent distortion in cross-range. Similarly, the range shift incurred by the scatterers must be smaller than the down-range resolution to prevent distortion in the down-range dimension. Blurring is observed whenever the Doppler shift of each scatterer deviates from a constant or if there is a rate of down-range change caused by acceleration, deceleration or turning [3].

Ideally, if the target has only uniform rotational motion and data is collected over a small angular aperture, then a simple Fourier transform process would bring a set of range profiles collected over a given dwell time (i.e., the coherent processing interval) into a focused two-dimensional image. However, actual targets observed by an operational radar rarely have such an ideal motion. Targets are often engaged in complicated maneuvers that combine translational and rotational motions. For long imaging times, i.e., long coherent integration time or for fast maneuvering targets, simple Fourier processing without compensation will lead to severe image blurring in cross-range. Therefore motion compensation is needed to generate focused ISAR imagery.

When an aircraft is in motion, small random perturbing rotational motions in pitch, roll and yaw are often produced. Unfortunately, these perturbed motions introduce distortion (e.g., blurring) in the ISAR images [4-5]. The observation of very large distortions from experimental ISAR data has been reported [6]. These observations clearly show that whenever an aircraft has a complex motion, such as pitching, yawing, rolling, the resulting ISAR image becomes severely distorted. It is very difficult to conduct a definitive study on the distortion phenomenon using in-flight aircraft. For example, there is no information on the location of the target rotational axis and no prior knowledge of the true (static) image of the target for comparison with the analysis. Therefore, we conducted a set of controlled experiments on the distortion of ISAR images in order to perform a systematic analysis of ISAR images [5]. A numerical model was developed to simulate the distorted ISAR images due to various time-dependent rotational motions that can occur in real in-flight targets [5]. This will allow us to gain new insights and a better understanding of the distortion phenomenon. In this paper, we use an adaptive joint time-frequency algorithm for re-focusing distorted ISAR images. This adaptive joint time-frequency algorithm is independently developed by the authors based on the concept introduced by [7-8]. The objective of this paper is to demonstrate the effectiveness of the adaptive joint time-frequency algorithm for motion compensation using both the simulated and experimental data sets. This study also adds insight into the distortion mechanisms that affect the ISAR images of a target in motion.

The paper is organized as follows. Section 2 presents an adaptive joint time-frequency procedure for extracting the phases of the prominent point-scatterers on the target from the radar data. In section 2.1, an adaptive search procedure and implementation are discussed. We show how the extracted phase information can be used in conjunction with the prominent point-processing model to achieve motion compensation. In section 3, we demonstrate this algorithm using both simulated and measured ISAR radar data. Conclusions are given in the last section.

2. ISAR Motion Compensation Algorithm

There are many different motion compensation algorithms that deal with target motion effects [1-2, 8-14]. Since target motion can always be decomposed into translational and rotational motion, a typical motion compensation algorithm consists of a two step process. First, a point on the target is focused through translational motion compensation. Note that when there is non-uniform rotational motion, other points on the target are not necessarily focused. Rotational motion compensation is then applied to focus these other points. If the rotational motion of the target is confined to a two-dimensional plane, rotational motion compensation of a second point on the target will focus the whole target.

When the coherent processing interval is long or when the target performs rapid maneuvers, the phase error due to the non-uniform rotational motion is often significant and must also be properly compensated. It has been shown that time-frequency analysis is an attractive way to address the Doppler tracking issue in motion compensation [15-18]. Specifically, it was shown that by applying the time-frequency distribution series in place of Fourier processing, the ISAR image can be effectively examined at each dwell time instant, thus eliminating range drift and Doppler smearing [15-19]. Unfortunately, the time-frequency distribution series is based on the Wigner-Ville distribution which does not preserve the phase information of the original image. Such information may be important for subsequent feature extraction or feature matching operations in target identification. Furthermore, the Doppler resolution achievable in this manner is still less than that offered by the total dwell time of the original data.

Recently, an adaptive joint time-frequency algorithm was introduced by [7-8] for phase estimation of prominent point scatterers based on the concept of signal parameterization [20-21]. In this method, the target motion is modeled as a polynomial function and an exhaustive search procedure is used to find the motion parameters that are embedded in the phase of the prominent point scatterers. Once the motion parameters are known, compensation of both translational and rotational effects can be achieved. In the following subsection, we describe the adaptive joint time-frequency algorithm for achieving both translational and rotational motion compensation. This algorithm is independently developed by the authors based on the concept described in [7-8].

2.1 Adaptive Search Procedure and Implementation

To form a focused image from raw radar data, it is customary to first carry out a coarse alignment of the data in the range dimension, followed by fine motion compensation in the cross-range dimension. Joint time-frequency techniques have been shown to be a useful tool for carrying out the fine motion compensation. A basic assumption is that the target is a rigid-body during the data acquisition time. When the target undergoes rigid-body motion, the resulting radar image preserves the spatial features of the target. The target is assumed to exhibit both translational and rotational motion. We assume that the standard range alignment has been applied to the data so that the coarse translational motion has been removed. That is, all the scatterers are located in their respective range cells. We assume that the rotational motion of the target is confined to a two-dimensional plane, i.e., with the fixed rotational axis, during the coherent processing interval. This type of target rotation is termed two-dimensional motion. When the target has a varying rotational axis (i.e., when the rotational motion is not confined to a two-dimensional plane), during the coherent processing interval, the target motion is termed three-dimensional motion [4, 22-24]. Since our measured data from controlled experiments is confined to a two-dimensional plane, we concentrate on the two-dimensional motion. However, we intend to address three-dimensional motion in a future publication.

When the target motion is confined to a two-dimensional plane during the imaging interval, the radar backscattered signal as a function of dwell time t (time index of each pulse) in a particular range cell x can be written as [7, 17]

$$s(x,t) = \sum_{k=1}^{N_k} A_k \exp\{-j\frac{4\pi f_0}{c}[R(t) + x_k\cos(\varphi(t)) + y_k\sin(\varphi(t))]\} \tag{1}$$

where N_k is the number of point-scatterers within range cell, f_0 is the center frequency of the radar and A_k is the the scattering magnitude. (x_k, y_k) denotes the kth point-scatterer position, where x_k represents the down-range and y_k represents the cross-range. $R(t)$ describes the residual uncompensated translational displacement and $\varphi(t)$ is the rotational displacement. After coarse range alignment, the residual uncompensated displacement is smaller than the range resolution, but it can still be larger than the radar wavelength. Therefore, either $R(t)$ or $\varphi(t)$ is no longer the simple constant or linear relationship which is assumed for ideal no-motion error ISAR imaging. They can be expanded into polynomial functions of the dwell time via Taylor series as

$$R(t) = R_0 + vt + \frac{1}{2!}v^{'}t^2 + \frac{1}{3!}v^{"}t^3... \tag{2}$$

$$\varphi(t) = \Omega t + \frac{1}{2!}\Omega^{'}t^2 + \frac{1}{3!}\Omega^{"}t^3... \tag{3}$$

By substituting these expressions into (1) and taking the first three terms, we obtain

$$s(x,t) = \sum_{k=1}^{N_k} A_k \exp\{-j\frac{4\pi f_0}{c}[a_0 + a_1 t + a_2 t^2 + ...]\} \tag{4}$$

where

$$
\begin{aligned}
a_0 &= R_0 + x_k, \\
a_1 &= v + y_k\Omega \quad \text{and} \\
a_2 &= \frac{1}{2}(v^{'} - x_k\Omega^2 + y_k\Omega^{'})
\end{aligned}
\tag{5}
$$

The constant phase term a_0 defines the coordinate positions of the scatterer on the target. The first-order phase term a_1 contains the radar line-of-sight translational motion and the constant rotational motion of the target. Note that the first-order phase term is a pure linear function of time. In this case a simple Fourier transform will focus the point-scatterers to their respective y_k positions in the cross-range dimension. The second-order and higher-order terms are the source of the phase error that cause image blurring. That is, any coefficients beyond the first-order are detrimental to ISAR image formation. It should be emphasized here that we assume $(\Omega t)^2 << 1$ so that this term can be neglected. This is generally a good approximation for CM (centimeter) and MM (millimeter) wave radars, as the angle window needed to form an image with sufficient cross-range resolution is comparatively small in absolute terms (i.e, a few degrees) [17]. With this approximation, the second-order coefficient becomes $a_2 = \frac{1}{2}(v^{'} + y_k\Omega^{'})$. The first term in a_2 represents the translational motion error and is independent of the cross-range y. The second term in a_2 represents the rotational motion error and is dependent on the cross-range y.

The simplified phase term in equation (4) can be considered as a sum of polynomials in the time series where the coefficients of each polynomial are determined by the coordinates of the scatterers and the target motion parameters. To solve the ISAR motion compensation problem, we need to determine these motion parameters and remove the unwanted non-linear phase terms from the radar data. Therefore, the goal of the motion compensation algorithm is to estimate and eliminate the second-order phase terms.

If the phase terms in the uncompensated radar signal are time-varying, the instantaneous frequency f_i of each of this components can be expressed as

$$
f_i = \frac{1}{2\pi}\frac{d\Phi(t)}{dt}
\tag{6}
$$

where $\Phi(t) = a_0 + a_1 t + a_2 t^2 + ...$

Therefore, the quadratic phase term in the uncompensated radar signal behaves like a linear chirp in the time-frequency plane. As shown in Figure 2a, the dwell time and Doppler frequency trajectories of the point-scatterers within a given range cell are straight lines. The displacement and slope of each line are related, respectively, to the linear and quadratic coefficients of their phase function. The task at hand is to determine these coefficients for the dominant point-scatterer within a range cell. This

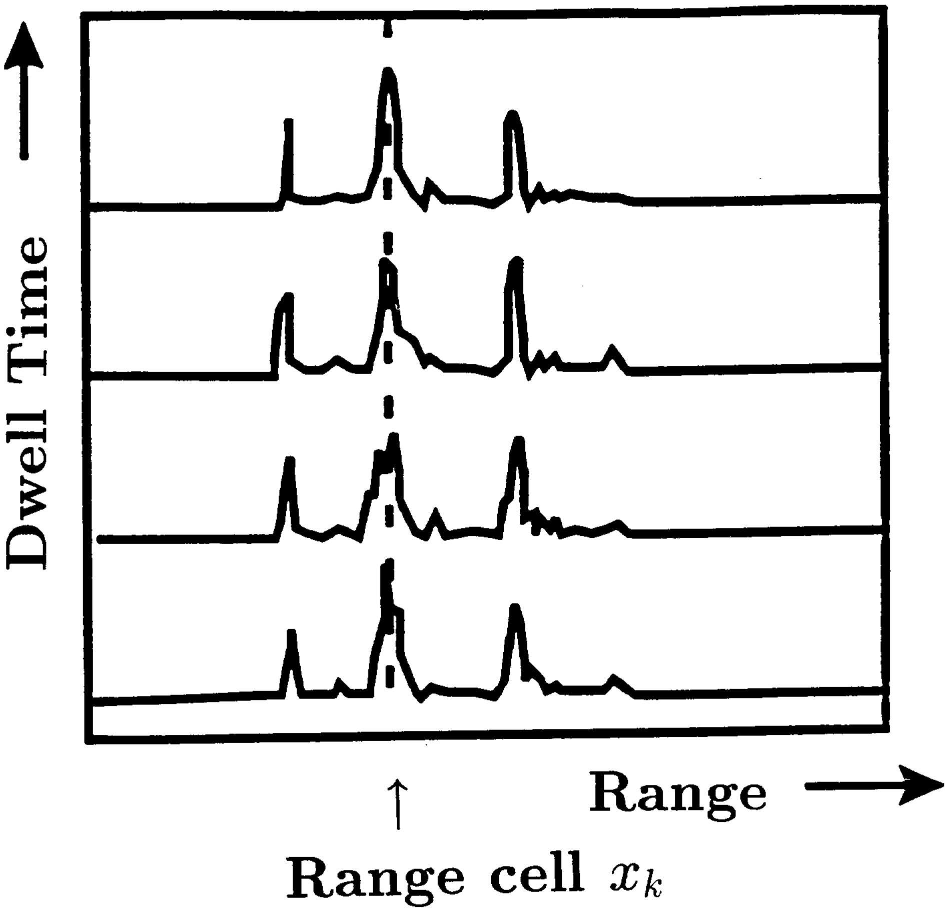

Figure 1: *Range profiles versus dwell time (or pulse number) after coarse range alignment.*

task can be accomplished using the adaptive joint time-frequency procedure. The essential idea of this procedure is to find the basis function that most resembles the strongest signal component in equation (1). For this problem, a basis function of the form

$$h_p(t) = \exp[-j\frac{4\pi f_0}{c}(f_1 t + \frac{1}{2}f_2 t^2 + \frac{1}{3}f_3 t^3 + ...)] \tag{7}$$

is used. The above set of basis function can be thought of as a collection of unit chirps, each with a different displacement and chirp slope [shown as a thick solid line in Figure 2b]. The best function is found by searching for parameters $f_1, f_2, f_3, ...$ that maximizes the projection from the radar signal onto the basis function. That is

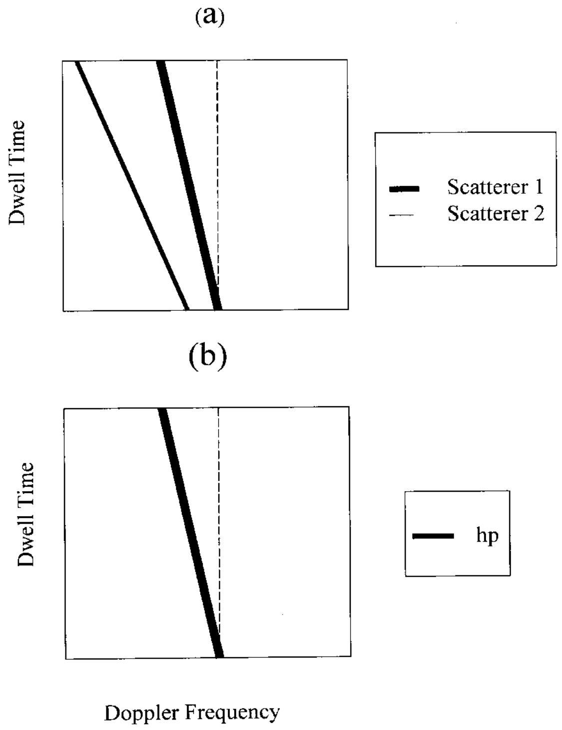

Figure 2: *Time-frequency representation of the signal in range cell* x_k*: (a) time-frequency display of the residual uncompensated radar signal of two prominent point-scatterers; and (b) the search procedure for the best basis* $h_p(t)$.

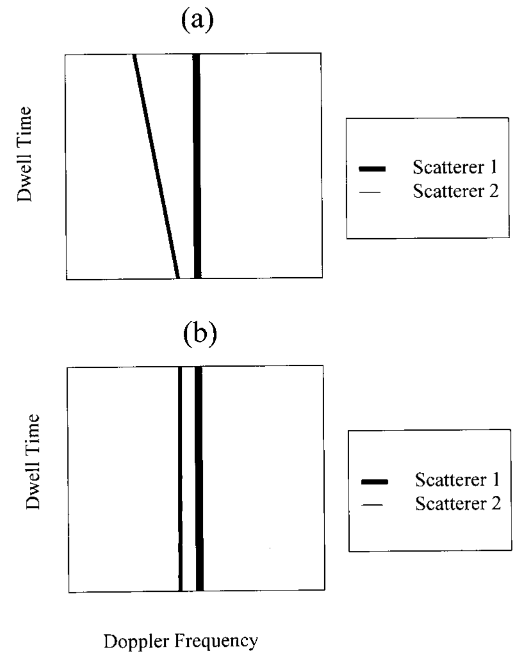

Figure 3: *Residual translation and rotational motion compensation by adaptive joint time-frequnecy: (a) after translation motion compensation using one promiment point-scatterer; and (b) after rotational motion compensation using a second prominent point-scatterer.*

$$\{f_1, f_2, f_3, ...\} = \arg\max |< s(x,t), h_p(t) >| \tag{8}$$

where the projection is formulated as the inner product of the two function as

$$|< s(x,t), h_p(t) >| = \int s(x,t) h_p^*(t) dt \tag{9}$$

Because of the rigid body assumption, the motion parameters in equation (5) are carried by every point-scatterer on the target. Equation (8) indicates that phase function parameters are estimated in a way that gives maximum projection from the radar data onto the basis function for that prominent point-scatterer. We choose to use only the dominant scatterer in a range cell in order to avoid estimation errors for the weaker scatterers. In the search procedure, the linear coefficient f_1 can efficiently be obtained by using the fast Fourier transform, while all other higher terms $f_2, f_3, ...$ are obtained by using exhaustive search techniques. In terms of performance, the algorithm is equivalent to picking out the strongest line in the time-frequency plane with the full Doppler resolution offered by the total coherent processing interval.

We illustrate the concept of adaptive joint time-frequency procedure for residual translational and rotational motion compensation in Figures 1, 2 and 3. The coarse range alignment is shown in Figure 1, where all the scatterers are located in the respective range cells. Range cell x_k contains a prominent point-scatterer and Figure 2a shows the time-frequency representation of the radar signal at this range cell. Each line in the time-frequency plane represents the time-varying Doppler characteristics of a scatter-center in the range cell. Each chirp represents an individual scatterer. If we assume there are only quadratic phase errors in the data, then the Doppler frequency shifts due to dwell time can be illustrated by linear chirps with different displacements and slopes. The displacement of the line represents the coefficient of the linear phase term and its slope represents the coefficient of the quadratic term. For higher-order phase errors, the radar signal of the scatterer in the time-frequency plane will not be a linear chirp but would be tilted and curved.

The goal of the adaptive joint time-frequency procedure is to find several strong chirp signals and extract their displacement and slope parameters. Figure 2b illustrates the best basis function h_p that resembles a strongest chirp signal in Figure 2a (scatterer 1). The best basis function is found by searching for parameters $f_1, f_2, f_3, ...$ that maximize the projection from the radar signal onto the basis function. Once the parameters $\{f_{11}, f_{12}, f_{13}, ...\}$ of the first prominent point-scatterer are found, the residual uncompensated translational displacement can be removed by multiplying the radar data with the conjugate of the ‘found’ basis function. The time-frequency display obtained at this stage is illustrated in Figure 3a. It should be noted that the strongest line has been straightened and shifted to the center of the Doppler frequency (cross-range) axis. Since all the point-scatterers share the same residual translation motion in equation (1), this operation will remove the residual translational motion of the whole target.

After the residual translation motion compensation, the backscattered signal in equation (1) becomes

$$s(t) = \sum_{k=1}^{N_k} A_k \exp\{-j\frac{4\pi f_0}{c}[\Delta x_k + \Delta y_k \varphi(t)]\} \tag{10}$$

where $(\Delta x_k, \Delta y_k)$ is the differential position of the kth scatterer relative to the prominent point-scatterer (i.e., (0,0)) chosen for residual translational motion compensation in the previous step. For rotational motion compensation, a second prominent point-scatterer, generally in a range cell different from the first one, is chosen for phase analysis. The same search procedure as described before is repeated for the rotational motion parameters $\{f_{21}, f_{22}, f_{23}, ...\}$ in equation (10). Then to remove the rotational motion, we define a new dwell time variable $t^{'}$ as

$$t^{'} = \frac{1}{f_{21}}(f_{22}t^2 + f_{23}t^3 + ...) \tag{11}$$

The radar data is now uniformly resampled in terms of this new time variable so that the phase of all point scatterers on the target depends linearly on time. The equation (10) now becomes

$$s(x, t^{'}) = \sum_{k=1}^{N_k} A_k \exp\{-j\frac{4\pi f_0}{c}[\Delta x_k + \Delta y_k \varphi(t^{'})]\} \tag{12}$$

If the phase is linearly dependent on time, then the residual motion due to non-uniform rotation rate is removed from the data. As we can see in the time-frequency display of Figure 3b, both lines are straightened, implying that all the quadratic phase errors are eliminated and that all the points are well-focused.

3. Results

We demonstrate the application and effectiveness of the adaptive joint time-frequency motion compensation procedure with simulated radar data and with measured experimental radar data. For simplicity, we consider either a stationary target or perfect translational motion compensation such that the radial velocity of the target is set to zero. In other words, we focus only on the rotational aspect of the target in forming the ISAR image.

3.1 Simulated Data

To gain a better physical insight into the scattering phenomenon of an aircraft's ISAR image, an aircraft can be assumed to be composed of a set of point scatterers on a two-dimensional plane. Each scattering point on the aircraft does not represent any geometric point on the target but a combination of scattering sources that return a radar echo. A two-dimensional model of an aircraft's scattering centers is sufficiently adequate to analyze the ISAR images of aircraft. In this simulation we assume the target contains six microwave corner reflectors (i.e., scatterers) to simulate the distorting effect that could occur in ISAR images.

We first test the adaptive joint time-frequency motion compensation algorithm on simulated radar data. Simulated radar data from six corner reflectors is used to demonstrate the adaptive joint time-frequency motion compensation procedure. A picture of the target is shown in Figure 4. The center frequency of the radar is 9 GHz and the bandwidth is 300 MHz. A total of 30 range cells and 50 cross-range cells are used for the imaging. In Figure 5, we show the image from the simulated data without any added motion error as a reference for comparison. This figure illustrates the undistorted ISAR image when the target is uniformly rotating at a constant rate of 3 degrees/second. Since there are no random motions, we can use the conventional Fourier transform; that is, we take a series of one-dimensional Fourier transforms across the target. As expected, the image is well-focused.

Then we inject perturbed random motion (or motion error) into the simulation. That is, in addition to the uniform (3 degrees/second) rotation we inject perturbed random motion through a 'sine-drive' by adding an additional sine wave to the motion. The resultant rotational motion will then be a non-uniform. It should be noted here that the rotational motion of the target is confined to a two-dimensional plane during the coherent processing interval. Figures 6a illustrates the distorted image obtained by using the conventional Fourier transform. In this case, the perturbed oscillation is 1 Hz. The figure clearly shows that the image is severely distorted, which means that target itself contains much rotational error. The image is smeared along the cross-range direction. This is because of the target's complex motion due to perturbed random motion during the entire coherent processing interval. The conventional radar imaging

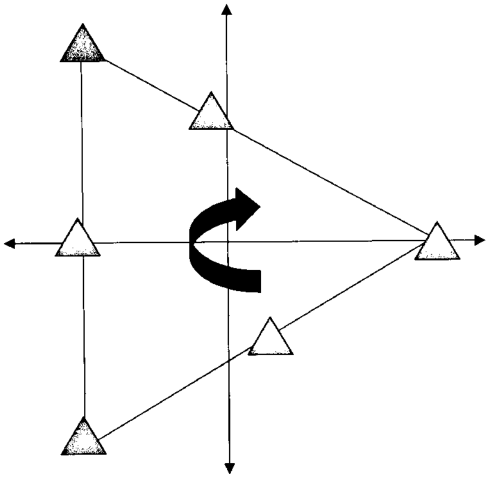

Figure 4: *A picture of the target contains six simulated corner reflectors.*

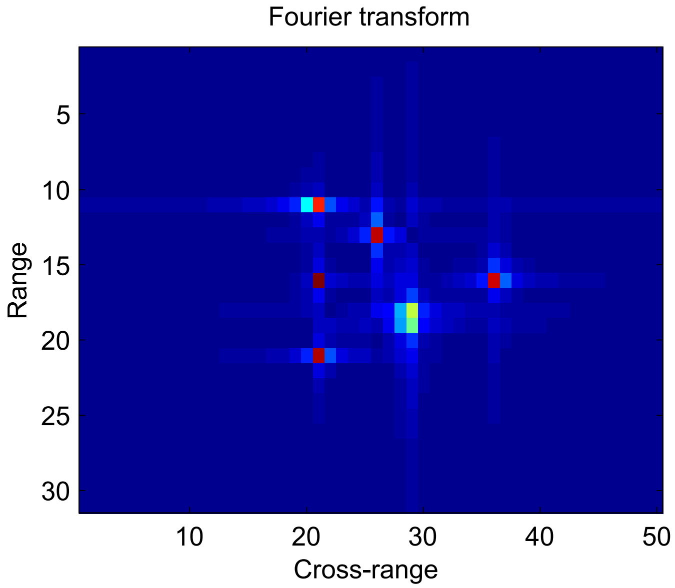

Figure 5: *Reference ISAR image of simulated corner reflectors data without any motion error.*

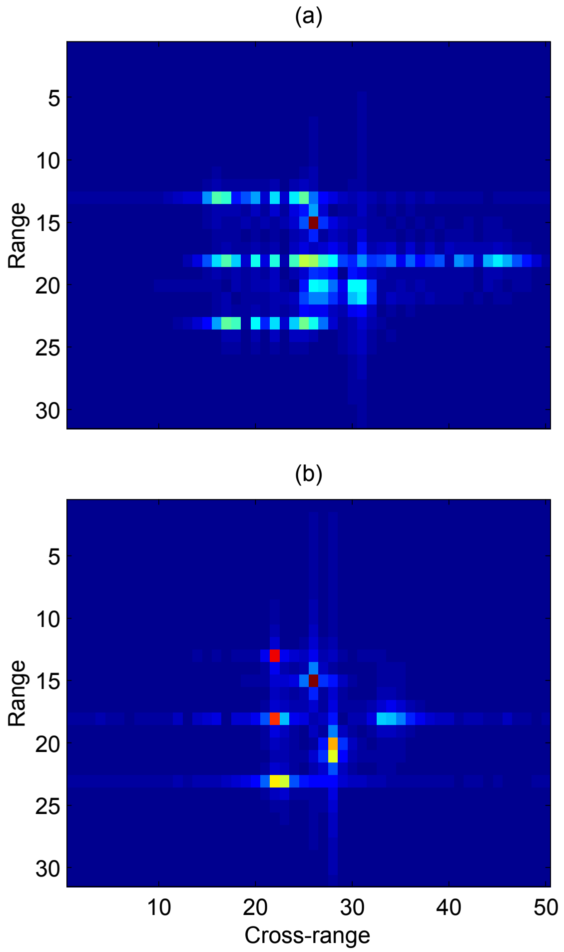

Figure 6: *ISAR image formation from simulated corner reflectors data: (a) ISAR image of simulated corner reflectors using conventional Fourier transform; (b) resulting final image after rotational motion compensation.*

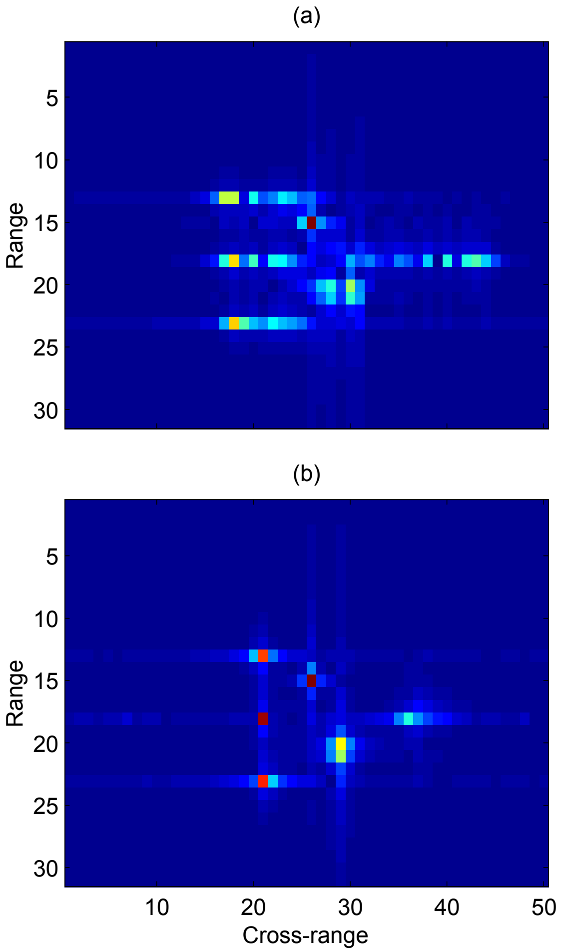

Figure 7: *ISAR image formation from experimental radar data: (a) ISAR image of measured corner reflectors using conventional Fourier transform; (b) resulting final image after residual rotational motion compensation.*

that uses Fourier transform, which works well for uniform rotational motion, cannot be directly applied to the perturbed target.

The adaptive joint time-frequency motion compensation algorithm is then applied to this data. Figure 6b illustrates the final image after the rotational motion compensation. All the scatterers are well focused in their individual range and cross-range cells. This implies that all the quadratic phase terms are eliminated.

Figure 7a illustrates another example of a distorted image due to perturbed random motion error. The image is poorly focused and the image of each scatterer is severely smeared. In this case, the perturbed oscillation is 0.57 Hz. Figures 7b shows that the adaptive joint time-frequency motion compensation algorithm successfully eliminates the quadratic phase terms and shows a well-focused ISAR image. In Figure 5, the image from the simulated data without any added motion errors is shown as a reference for comparison. We can see that the motion-compensated image achieves the same sharpness as the reference image.

3.2 Experimental Data

We conducted an experimental study to investigate the distortion of ISAR images of moving targets, to develop a numerical model simulation to characterize the distortion behavior and to examine the time-frequency techniques for restoring distorted ISAR images and to verify our simulated results.

A 5m by 5m delta-wing apparatus was constructed to simulate a full size target. A picture of the target is shown in Figure 8. Six corner reflectors were mounted on the apparatus to simulate the major scattering centers of the target. These six corner reflectors were set to oscillate on their own at a controlled rate to simulate the fluttering effect from aircraft parts or mounted stores on aircraft. The apparatus was mounted on a rotating/heaving table that can produce rotational motions at a controlled rate. These rotational motions were confined to a two-dimensional plane. Therefore, data from this pseudo point-source target permits an easier and a more definitive analysis of the residual motion effects on ISAR images.

The radar data was collected using a ground radar having a center frequency of 9.05 GHz and a bandwidth of 300 MHz. A total of 50 range cells and 50 cross-range cells are used for the imaging. To demonstrate the effectiveness of the adaptive joint time-frequency motion compensation algorithm, we tested our algorithm on two measured radar data sets. We apply both the Fourier-based and time-frequency-based image formation to a set of measured radar data.

The first measured data set contains non-uniform rotational motion in which the perturbed random motion is less than 1 Hz. Figure 9a shows the resulting ISAR image from taking a series of one-dimensional Fourier transforms across the dwell time. Since significant phase errors due to non-uniform rotational motion exist in the data, the image is quite blurred in the Doppler dimension. It is not possible to distinguish

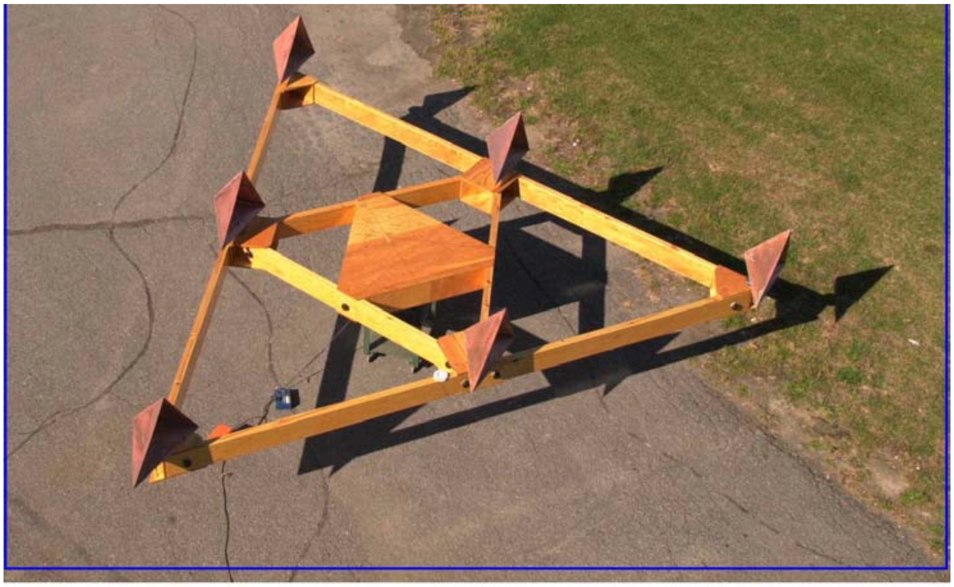

Figure 8: *A picture of the target motion simulator experimental apparatus.*

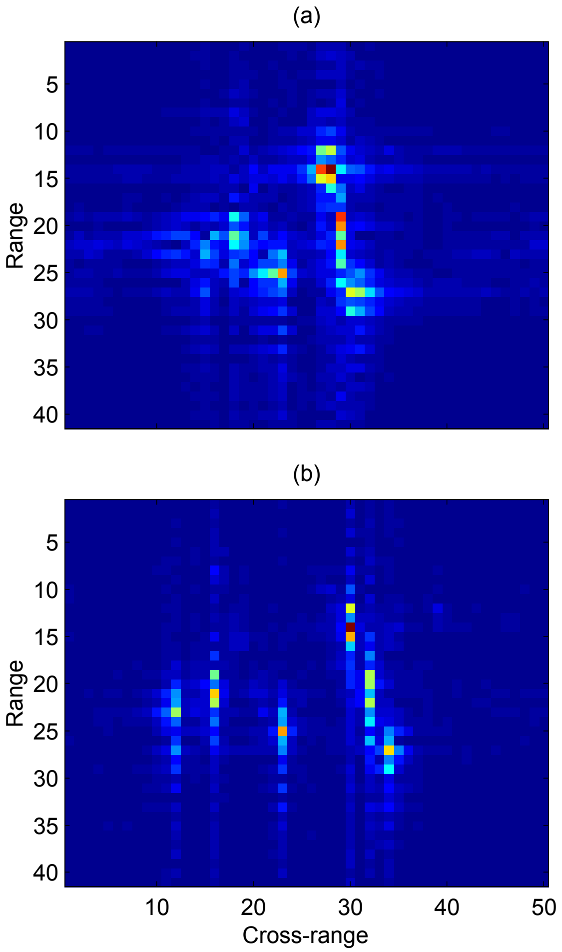

Figure 9: *ISAR image formation from experimental radar data: (a) ISAR image of measured corner reflectors using conventional Fourier transform; (b) resulting final image after rotational motion compensation.*

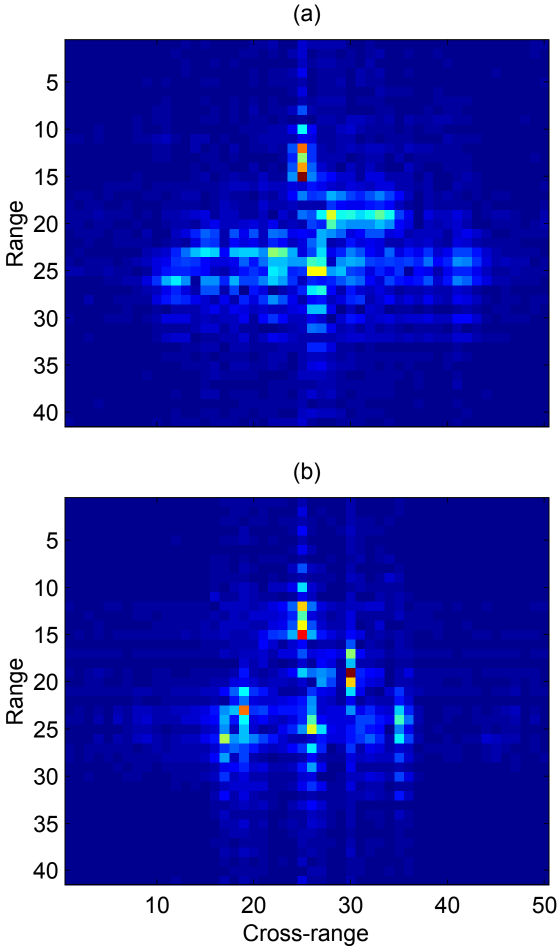

Figure 10: *ISAR image formation from experimental radar data: (a) ISAR image of measured corner reflectors using conventional Fourier transform; (b) resulting final image after residual rotational motion compensation.*

individual scatterers because some of the scatterers are severely blurred. We then applied the adaptive joint time-frequency motion compensation algorithm on the data. Figure 9b illustrates the final image after the rotational motion compensation. All the corner reflectors are well-focused in the image. That is, the image is focused in range and cross-range.

The second measured data set contains non-uniform rotational motion in which the perturbed random motion is more than 1 Hz. Figure 10a illustrates the resulting image after taking a series of one-dimensional Fourier transform across the dwell time. This image is very severely distorted and scatterers are indistinguishable from one another. The image is severely blurry in the Doppler dimension. The fuzzy image clearly shows that significant amount of rotational motion errors exist in the data. Figure 10b shows the final image after the rotational motion compensation. The Doppler smearing is significantly reduced and the image shows dramatic improvement over that shows in Figure 10a. The image is now focused and the six corner reflectors of the target are clearly visible. We see that the adaptive joint time-frequency motion compensation algorithm performed well in achieving a focused image of the target. It should be noted that these results are preliminary and more data has to be analyzed to evaluate the consistency of adaptive joint time-frequency motion compensation algorithm. We intend to do this in the near future.

One drawback of the adaptive joint time-frequency method is the computational burden associated with the exhaustive search procedure for the motion parameters. This problem becomes especially severe when higher-order motion effects are involved. Recently, generic algorithms have been attempted as a way to reduce the computational complexity and speed up the search procedure [25-26].

4. Conclusion

An adaptive joint time-frequency algorithm has been applied and evaluated for focusing distorted ISAR (inverse synthetic aperture radar) images when the target motion is confined to a two-dimensional plane. It is shown that the adaptive joint time-frequency algorithm provides an effective method of achieving rotational motion compensation for ISAR imaging. Examples provided demonstrate the effectiveness of the adaptive joint time-frequency algorithm with both simulated and experimental ISAR data. Results show that if a target is moving smoothly, standard motion compensation generates a clear image of the target by using the conventional Fourier transform methods. However, when a target performs complex motion such as perturbed random motions, standard motion compensation is not sufficient to generate an acceptable image. In this case, the adaptive joint time-frequency algorithm provides an efficient candidate to resolve the image smearing caused by the time-varying behavior and leads to a well-focused ISAR image when the target motion is confined to a two-dimensional plane. This study also adds insight into the distortion mechanisms that affect the ISAR images of a target in motion.

References

1. Ausherman, A., Kozma, A., Waker, J. L., Jones, H. M., and Poggio, E. C. (1984). Development in radar imaging, *IEEE Trans. Aerospace Electron. Syst.*, vol 20, pp. 363-400
2. Chen, C. C., and Andrews, H. C. (1980). Target motion induced radar imaging, *IEEE Trans. Aerospace Electron. Syst.*, vol. 16, pp. 2-14
3. Son, J. S., Thomas, G., and Flores, B. C. (2000). Range-Doppler radar imaging and motion compensation *Artech House*, Boston, MA, USA
4. Chen, V. C., and Miceli, W. J. (1999). Effect of roll, pitch and yaw motions on ISAR imaging, *SPIE Proc. on Radar Processing*, vol. 3810, pp. 149-158
5. Wong, S. K., Duff, G., and Riseborough, E. (2001). Analysis of distortion in the high range resolution profile from a perturbed target, *IEE Proc.-Radar, Sonar Navig.*, vol 148, pp. 353-362
6. Sparr, T., Hamran, S.-E., and Korsbakken, E. (2000). Estimation and correction of complex target motion effects in inverse synthetic aperture imaging of aircraft, *IEEE radar 2000 conference*, Alexandra, USA
7. Ling, H., Wang, Y., and Chen, V. C. (1997). ISAR image formation and featue extraction using adaptive joint time-frequency processing, *SPIE Proc. on Wavelet applications,* vol. 3708, pp. 424-432
8. Wang, Y., Ling, H., and Chen, V. C. (1998). ISAR motion compensation via adaptive joint time-frequency technique, *IEEE Trans. Aerospace and Electron. Syst.*, Vol. 34, pp. 670-677
9. Jain, A., and Patel, I. (1992). SAR/ISAR imaging of a nonuniformly rotating targets, *IEEE Trans. Aerospace Electron. Syst.*, vol. 28, pp 317-321
10. Colloway, T. M., and Donohoe, G. W. (1992). Sub-aperture autofocus for synthetic aperture radar, *IEEE Trans. Aerospace Electron. Syst.*, vol. 30, pp. 617-621
11. Itoh, T., Sueda, H., and Watanabe, Y. (1996). Motion compensation for ISAR via centroid tracking, *IEEE Trans. Aerospace Electron. Syst.*, vol. 32, pp. 1191-1197
12. Carrara, W. G., Goodman, R. S., and Majewski, R. M. (1995). Spotlight synthetic aperture radar - signal processing and algorithms, *Artech House*, Boston, MA, USA
13. Rihaczek, A. W., and Hershkowitz, S. J. (1996) Radar resolution and complex-image analysis *Artech House*, Boston, MA, USA
14. Werness, S., Carrara, W., Joyce, L., and Franczak, D. (1990). Moving target imaging algorithms for SAR data, *IEEE Trans. Aerospace Electron. Syst.*, vol. 26, pp. 57-67

15. Chen, V. C. (1995). Reconstruction of inverse synthetic aperture images using adaptive joint time-frequency wavelet transforms, *SPIE Proc. on wavelet application,* vol. 2491, pp. 373-386

16. Chen, V. C., and Qian, S. (1998). Joint time-frequency transform for radar range-Doppler imaging, *IEEE Transactions on Aerospace and Electronic Systems*, Vol. 34, No. 2, pp. 486-499

17. Chen, V. C., and Ling, H. (2002). Time-Frequency Transforms for Radar Imaging and Signal Analysis, *Artech House*, Boston, MA, USA

18. Qian, S., and Chen, D. (1996). Joint time-frequency analysis: methods and applications, *Prentice-Hall Inc.,* New York, USA

19. Qian, S., and Chen, D. (1994). Decomposition of the Wigner-Ville distribution and time-frequency distribution series. *IEEE Trans. Aerospace Electron. Syst.*, vol. 42, pp. 2836-2842

20. Qian, S., and Chen, D. (1994). Signal representation using adaptive normalized Gaussian functions, *Signal processing,* vol. 36, pp. 1-11

21. Mallat, S. G., and Zhang, Z. (1993). Matching pursuits with time-frequency dictionaries, *IEEE Trans. Signal Processing*, vol. 41, pp. 3397-3415

22. Li, J., Ling, H., and Chen, V. C. (2001). An alogorithm to detect the presence of 3D target motion from ISAR data, *Multimensional Systems and Signal Processing*, Special issue on radar signal processing and its applications

23. Li, J., and Ling, H. (2001). 3D ISAR image reconstruction of a target with motion data using adaptive feature extraction *J. Electromag. Waves Applications*, vol. 15, pp. 1571-1587

24. Li, J., Wang, Y., Bhalla, R., Ling, H., and Chen, V. C. (1999). Comparison of high-resolution ISAR imagery from measured data and synthetic signatures, *SPIE Proc. on Radar Processing*, vol. 3810, pp. 170-179

25. Goldberg, D. E. (1989). Genetic algorithms in search, optimization and machine learning, *Addison-Wesley*, Reading, MA, USA

26. Li, J., and Ling, H. (2001). ISAR motion detection and compensation using genetic algorithms, *SPIE Proc. on Wavelet Applications VIII*, vol. 4391. pp. 380-388

DOCUMENT CONTROL DATA

(Security classification of title, body of abstract and indexing annotation must be entered when the overall document is classified)

1. ORIGINATOR (the name and address of the organization preparing the document. Organizations for whom the document was prepared, e.g. Establishment sponsoring a contractor's report, or tasking agency, are entered in section 8.) Defence R&D Canada - Ottawa Ottawa, Ontario, Canada K1A 0Z4	2. SECURITY CLASSIFICATION (overall security classification of the document, including special warning terms if applicable) UNCLASSIFIED

3. TITLE (the complete document title as indicated on the title page. Its classification should be indicated by the appropriate abbreviation (S,C or U) in parentheses after the title.)

Focusing ISAR Images Using Adaptive Joint Time-Frequency Algorithm on Simulated and Experimental Radar Data (U)

4. AUTHORS (Last name, first name, middle initial)

Thayaparan, Thayananthan;Wong, Silvester; Riseborough, Edwin; Lampropoulos, George

5. DATE OF PUBLICATION (month and year of publication of document) March 2003	6a. NO. OF PAGES (total containing information. Include Annexes, Appendices, etc.) 32	6b. NO. OF REFS (total cited in document) 26

7. DESCRIPTIVE NOTES (the category of the document, e.g. technical report, technical note or memorandum. If appropriate, enter the type of report, e.g. interim, progress, summary, annual or final. Give the inclusive dates when a specific reporting period is covered.)

DRDC Ottawa TECHNICAL MEMORANDOM

8. SPONSORING ACTIVITY (the name of the department project office or laboratory sponsoring the research and development. Include the address.)

Defence R&D Canada - Ottawa
Ottawa, Ontario, Canada K1A 0Z4

9a. PROJECT OR GRANT NO. (if appropriate, the applicable research and development project or grant number under which the document was written. Please specify whether project or grant) 11ar16	9b. CONTRACT NO. (if appropriate, the applicable number under which the document was written)
10a. ORIGINATOR'S DOCUMENT NUMBER (the official document number by which the document is identified by the originating activity. This number must be unique to this document.) DRDC Ottawa TM 2003-089	10b. OTHER DOCUMENT NOS. (Any other numbers which may be assigned this document either by the originator or by the sponsor)

11. DOCUMENT AVAILABILITY (any limitations on further dissemination of the document, other than those imposed by security classification)

(X) Unlimited distribution
( ) Distribution limited to defence departments and defence contractors; further distribution only as approved
( ) Distribution limited to defence departments and Canadian defence contractors; further distribution only as approved
( ) Distribution limited to government departments and agencies; further distribution only as approved
( ) Distribution limited to defence departments; further distribution only as approved
( ) Other (please specify):

12. DOCUMENT ANNOUNCEMENT (any limitation to the bibliographic announcement of this document. This will normally correspond to the Document Availability (11). However, where further distribution (beyond the audience specified in 11) is possible, a wider announcement audience may be selected.)

13. ABSTRACT (a brief and factual summary of the document. It may also appear elsewhere in the body of the document itself. It is highly desirable that the abstract of classified documents be unclassified. Each paragraph of the abstract shall begin with an indication of the security classification of the information in the paragraph (unless the document itself is unclassified) represented as (S), (C), or (U). It is not necessary to include here abstracts in both official languages unless the text is bilingual).

(U) When target motion is confined to a two-dimensional plane during coherent processing intervals, the adaptive joint time-frequency algorithm is shown to be an effective method for achieving rotational motion compensation in ISAR imaging. We illustrate the algorithm using both simulated and measured experimental radar data sets. The results show that the adaptive joint time-frequency algorithm performed very well in achieving a focused image of the target. Results also demonstrate that adaptive joint time-frequency techniques can significantly improve the distorted ISAR image over what can be achieved by conventional Fourier transform methods when the rotational motion of the target is confined to a two-dimensional plane. This study also adds insight into the distortion mechanisms that affect the ISAR images of a target in motion.

14. KEYWORDS, DESCRIPTORS or IDENTIFIERS (technically meaningful terms or short phrases that characterize a document and could be helpful in cataloguing the document. They should be selected so that no security classification is required. Identifiers such as equipment model designation, trade name, military project code name, geographic location may also be included. If possible keywords should be selected from a published thesaurus. e.g. Thesaurus of Engineering and Scientific Terms (TEST) and that thesaurus-identified. If it is not possible to select indexing terms which are Unclassified, the classification of each should be indicated as with the title.)

Time-Frequency Distribution
High Range Resolution
Inverse Synthetic Aperture Radar
Non-Cooperative Target Recognition
Fourier Transform
Prominent Point Scatterers
Doppler Smearing
Motion Compensation
ISAR image

Defence R&D Canada

Canada's leader in defence
and national security R&D

R & D pour la défense Canada

Chef de file au Canada en R & D
pour la défense et la sécurité nationale

www.drdc-rddc.gc.ca